BBA - Bioenergetics 1860 (2019) 499–507

Contents lists available at ScienceDirect

BBA - Bioenergetics

journal homepage: www.elsevier.com/locate/bbabio

Single-molecule microscopy studies of LHCII enriched in Vio or Zea

Marijonas Tutkus[a], Francesco Saccon[c], Jevgenij Chmeliov[a,b], Oskaras Venckus[a], Ignas Ciplys[a], Alexander V. Ruban[c], Leonas Valkunas[a,b,*]

[a] Department of Molecular Compound Physics, Center for Physical Sciences and Technology, Sauletekio Ave. 3, LT-10257 Vilnius, Lithuania
[b] Institute of Chemical Physics, Faculty of Physics, Vilnius University, Sauletekio Ave. 9, LT-10222 Vilnius, Lithuania
[c] The School of Biological and Chemical Sciences, Queen Mary, University of London, Mile End Road, London E1 4NS, UK

A B S T R A C T

Plants have developed multiple self-regulatory mechanisms to efficiently function under varying sunlight conditions. At high light intensities, non-photochemical quenching (NPQ) is activated on a molecular level, safely dissipating an excess excitation as heat. The exact molecular mechanism for NPQ is still under debate, but it is widely agreed that the direct participation of the carotenoid pigments is involved, one of the proposed candidate being the zeaxanthin. In this work, we performed fluorescence measurements of violaxanthin- and zeaxanthin-enriched major light-harvesting complexes (LHCII), in ensemble and at the single pigment–protein complex level, where aggregation is prevented by immobilization of LHCIIs onto a surface. We show that a selective enrichment of LHCII with violaxanthin or zeaxanthin affects neither the ability of LHCII to switch into a dissipative conformation nor the maximal level of induced quenching. However, the kinetics of the fluorescence decrease due to aggregation on the timescale of seconds are different, prompting towards a modulatory effect of zeaxanthin in the dynamics of quenching.

1. Introduction

Oxygenic photosynthesis is one of the most important physiological processes occurring in Earth biosphere, during which solar energy is stored in a form of chemical bonds and the atmosphere is refilled with oxygen as a by-product of photosynthetic reactions. The photosynthetic apparatus of green plants is highly optimized to perform efficiently under varying environment conditions [1]. The spectral properties and mutual arrangement of chlorophylls (Chls) and carotenoids(Car) within the pigment-protein complexes and of the latter within the photosynthetic units ensure efficient light harvesting in dim light followed by the excitation energy transfer towards the reaction center. Such efficiency, however, might be fraught with the photo-damage to photosystem II (PSII) induced by the over-excitation of the light-harvesting antenna when it is exposed to excess light [1]. Over billions of years of evolution, plants have developed multiple self-regulatory mechanisms to deal with this threat. A fast and efficient one, acting on a molecular level and safely dissipating excess excitation energy as heat, is known as an energy-dependent (qE) component of the non-photochemical quenching (NPQ) [2,3].

The extensive studies performed over the past two decades have revealed that NPQ arises from structural changes in the light harvesting antenna that can be reversibly activated within seconds to minutes in response to the increase of ΔpH across the thylakoid membrane during the bright sunlight [3]. The presence and protonation of the PsbS protein were identified to be required for NPQ activation [3–5], and total NPQ efficiency is enhanced by the conversion of the xanthophyll violaxanthin (Vio) into zeaxanthin (Zea), through the intermediate antheraxanthin, by the Vio de-epoxidase (VDE, the so-called xanthophyll cycle) [6]. The exact molecular mechanism for NPQ is still under debate, but it is widely agreed that the direct participation of the Car pigments is involved [7–11]. The main candidate for the NPQ location is the major light-harvesting complex of photosystem II (LHCII), even though minor antenna complexes have also been considered [3,12,13].

LHCII is a trimeric transmembrane protein rich in chromophores (Fig. 1). Its crystal structure, known with the sub-3 Å resolution [14], reveals that each monomeric subunit contains eighteen pigment molecules: six Chls *b*, eight Chls *a*, and four Cars, namely two luteins (located in Lut1 and Lut2 binding sites), violaxanthin in V1 site, and neoxanthyn (Neo) in N1 site. Both luteins are arranged in a cross pattern in the center of LHCII monomer, assist in holding the whole protein scaffold together and are responsible for the trimerisation of the LHCII [15]. They were also proposed to participate in NPQ via incoherent excitation energy transfer from the nearby Chls to the optically dark short-lived S_1 states of Luts [8,16,17]. On the other hand, Vio is located on a periphery of the LHCII trimer, which makes it easily accessible for the Vio de-epoxidase to convert it into Zea [14,18].

The link between qE and the xanthophyll cycle carotenoids is still one of the most uncertain aspects in the NPQ scenario. The reversible de-epoxidation of violaxanthin to zeaxanthin and its dependency on

* Corresponding author.
E-mail address: leonas.valkunas@ff.vu.lt (L. Valkunas).

https://doi.org/10.1016/j.bbabio.2019.05.002
Received 23 February 2018; Received in revised form 20 December 2018; Accepted 6 January 2019
Available online 02 May 2019

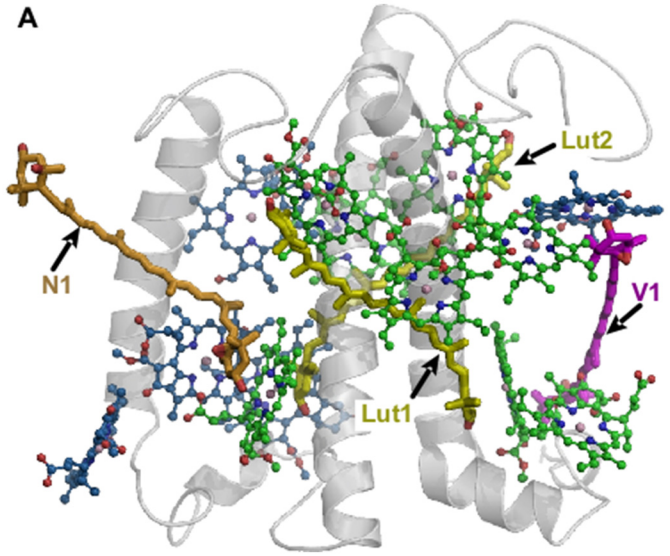

Fig. 1. Crystal structure of LHCII monomer (PDB ID: 1RWT) and carotenoid binding sites (Lut1, Lut2, V1 and N1). Protein scaffold in grey, Chl *a* in green, Chl *b* in blue, both luteins in dark yellow, xanthophyll cycle carotenoid (Vio/Zea) in magenta, Neo in orange. (For interpretation of the references to color in this figure legend, the reader is referred to the web version of this article.)

illumination is a long-known aspect of the photosynthetic membrane [19,20]. However, it was only in the 90s that the work of Demmig-Adams elucidated a link between this physiological trait and the process of non-photochemical quenching of chlorophyll fluorescence [6]. This finding ignited an elegant hypothesis put forward by Frank and coworkers, according to which the de-epoxidation of violaxanthin during high light lowers the energy of the xanthophyll's first excited state so that it becomes accessible for excitation energy transfer from chlorophylls [21]. In this way, zeaxanthin can act directly as a quencher of the excited state of chlorophylls. Later, it was found that the S_1 energy level of both Vio and Zea lies below the energy of chlorophyll S_1, therefore confuting the de-epoxidation as the sole factor for the appearance of the quencher [22]. However, more recently, evidences of a reductive-type of quenching, where Zea cations are formed in illuminated thylakoids, have been found [7,10,23,24]. Snapshot transient absorption data have also suggested that a stronger coupling of Chl and Zea during NPQ conditions allow excitation energy transfer from Chl to Zea to occur [7,23]. Based on these observations, a direct role of Zea in qE was suggested, with the minor antenna proposed as one of the NPQ sites [10,12]. However, it has been questioned the extent to which the formation of Zea^+ cation is correlated with qE and how much minor antenna are involved since neither the presence of Zea or minor antennae are strict requirements for the formation of qE. Observations of the hysteretic correlation between trans-membrane ΔpH and qE in the presence of Vio or Zea have prompted to a particular role of the xanthophyll cycle carotenoids as allosteric regulators of qE [24,25]. It was indeed demonstrated that isolated major LHCII complexes with Zea in the reaction mixture accelerated the drop in fluorescence quantum yield under the NPQ-mimicking conditions, while violaxanthin retarded this process rather than simply inhibiting it [26]. Also, it has been shown that when lumen pH drops below 5, Zea is not prerequisite for qE formation [18]. Therefore, it is possible that in vivo zeaxanthin thermodynamically favors the aggregation of antenna complexes, which in turn stabilizes the quenched conformation of the pigment–protein complexes [24,27].

As a result, the role of Zea in plant self-regulation is yet to be fully understood: it might be that Zea induces a photo-physical effect, when this carotenoid directly quenches chlorophyll excited state, or a physico-chemical effect, when it indirectly assists the quenching process by stabilizing the corresponding structural changes within the light-harvesting antenna. Similarly, it is still debated whether Zea effect is exerted at the single-molecule or ensemble level [28,29]. To assess these questions and study the role of Zea in excitation energy quenching in the LHCII complexes, targeted mutagenesis has been widely used previously to block biosynthesis of Vio and thus produce LHCII complexes with zeaxanthin in the V1 binding site. Alternative approach is to mimic natural NPQ condition by inducing Vio de-epoxidation in the wild type plants followed by the purification of the pigment–proteins, thus obtaining naturally Zea-enriched LHCII complexes [28,30]. In this work, we used the LHCII trimers obtained in the latter way and performed their fluorescence (FL) measurements, in ensemble and at the single pigment–protein complex level, where aggregation is prevented by immobilization of LHCIIs onto a surface, to compare their quenching ability with the naturally Vio-enriched LHCII complexes. We show that a selective enrichment of LHCII with violaxanthin or zeaxanthin affects neither the intrinsic ability of LHCII to switch into a dissipative conformation nor the maximum quenching inducible. However, the kinetics of the fluorescence decrease due to LHCII aggregation on the time scale of seconds are different, prompting towards a modulatory effect of zeaxanthin in the dynamics of quenching.

2. Methods

2.1. LHCII isolation and characterization

For preparation of unstacked thylakoids, spinach leaves from supermarket were used. Fresh leaf tissue was homogenized in ice-cold grinding medium (330 mM sorbitol, 10 mM $Na_4P_2O_7$, pH 6.5) with a polytron blender. The homogenate was then filtered through four layers of muslin followed by four layers of muslin and one layer of cotton wool. The filtrate was centrifuged for 10 min at 4000 ×*g*, and the chloroplast-enriched pellet was resuspended in wash buffer (330 mM sorbitol, 10 mM MES, pH 6.5), followed by another 10-min centrifugation at 4000 ×*g*. The pellet was then resuspended in a resuspension medium (330 mM sorbitol, 1 mM EDTA, 50 mM HEPES, pH 7.6) and breaking medium (10 mM HEPES, pH 7.6) was added to lyse any remaining intact chloroplasts. After 30 s, an equal volume of osmotic medium (660 mM sorbitol, 40 mM MES, pH 6.5) was added to restore the right osmotic potential. After centrifugation, thylakoids were resuspended in a small volume of resuspension medium.

Induction of maximum de-epoxidation of violaxanthin was performed as described before [31]. Briefly, spinach leaves were treated with 900 μE of light for 1 h, keeping the petioles submersed in cold water with a constant flux of nitrogen. 3 mM D-isoascorbate was added to grinding medium during thylakoid preparation. Thylakoids in resuspension medium where diluted to a chlorophyll concentration of 150 μg/ml, incubated for one hour at room temperature in 330 mM sorbitol, 25 mM HEPES, 25 mM Na-citrate, 40 mM Na-ascorbate, pH 5.5, and centrifuged 10 min at 4000 ×*g*. Thylakoids were then resuspended in a small volume of resuspension medium.

Solubilisation of thylakoid membranes was performed with β-DM detergent, on ice, with occasional mixing, with 25 mM β-DM (β-DM/Chl = ~13). Fractionation of protein complexes was performed with seven steps exponential sucrose gradient, as previously described [30], with a buffer containing 25 mM HEPES, 200 μM β-DM at pH 7.8.

2.2. Quenching induction assay

To monitor fluorescence quenching in solution, isolated LHCII were diluted in a buffer containing 10 mM tri-sodium citrate, 10 mM HEPES, pH 5.5 (final chlorophyll concentration, 3 μg/ml; final detergent concentration, 6 μM). Chlorophyll *a* fluorescence traces were recorded with a Dual-PAM 100 (Walz GmbH, Effeltrich, Germany) as described previously [32]. During this procedure, chlorophyll *a* fluorescence traces (integrated intensity of wavelength range of > 700 nm) were recorded

using a 460 nm measuring beam (24 μmol photons $m^{-2} s^{-1}$). The experiments were performed at room temperature under continuous stirring. Data represent the averages of 3 experiments, and are plotted from the moment of injection of the LHCII in the buffer. Normalization was done on the initial maximum of Chl fluorescence.

2.3. Fluorescence lifetime measurements

Fluorescence lifetime values were measured with time-correlated single photon counting (TCSPC), performed using a FluoTime 200 fluorometer (PicoQuant, Germany). Fluorescence lifetime decay kinetics were measured on diluted LHCII (3 μg/ml total chlorophyll content). Excitation was provided by the 468 nm laser diode at 20 MHz repetition rate and 0.6 mW (~30 pJ/pulse) intensity. Fluorescence was detected at 680 nm with 2 nm of slit width.

FluoFit software (PicoQuant, Germany) was used to analyze fluorescence lifetime data by a multi-exponential model with iterative reconvolution of the instrument response function (IRF, 50 ps). The χ^2 parameter and autocorrelation function were used to judge the quality of the fit. Average lifetimes were calculated as $\Sigma_i(A_i \cdot \tau_i) / \Sigma_i A_i$, where A_i is the amplitude of *i*-th lifetime component and τ_i is the respective fluorescence lifetime value.

2.4. Steady-state spectroscopy

Fluorescence emission spectra of LHCII (3 μg/ml total chlorophyll content) were recorded at 77 K using a Jobin Yvon FluoroMax-3 spectrophotometer equipped with a liquid-nitrogen-cooled cryostat, as previously described [13]. Excitation was performed at 435 nm with 5 nm slit width and the fluorescence spectral resolution was 0.5 nm. Integration time was set to 0.1 s. Every spectrum is the average of 5 scans. Spectra were normalized at their absolute maximum.

Absorption spectra of LHCII (10 μg/ml total chlorophyll content) were recorded with an Aminco DW- 2000 UV/Vis spectrophotometer (Olis Inc., USA), in dual-beam mode as previously described. Slits width was 0.5 mm and the spectral bandwidth 2 nm. Traces were normalized at the maximum of the Soret absorption band of Chl *a*.

2.5. Pigment analysis

Pigment quantification was performed through reversed-phase HPLC, using a LiChrospher 100-RP-18 column (Merck) and a Dionex Summit chromatography system as described previously [24]. Samples were solubilized in 80% ice-cold acetone, centrifuged for 1 min and filtered through a 0.22 μm filter. The solvents used were: acetonitrile, methanol, 0.1 M filtered Tris, pH 8 (A) and 80% methanol, 20% hexane (B). The run profile was: 0–9 min A, 9–12.5 min A/B gradient, 12.5–18 min B. Each peak was integrated using the Chromelion software and pigment concentration was estimated using standards of known concentration.

2.6. Streak camera measurements

Time-resolved fluorescence dynamics of the samples were measured as described previously [33]. Briefly, we used Hamamatsu C5680 streak camera with M5677 single-sweep module coupled to a spectrometer. Femtosecond Yb:KGW oscillator (Pharos, Light Conversion Ltd.) with a frequency doubler (HIRO, Light Con- version Ltd.) producing 515 nm sub-100-fs pulses at a 76 MHz repetition rate was employed, and a pulse picker was used to reduce the repetition rate to 20 kHz for nanosecond timescales. The beam was attenuated down to about 100 pJ per pulse and focused into about 100 μm spot on the sample. The temporal resolution of the whole system was ~90 ps. All the measurements were performed at the room temperature in a fused silica cell of 0.1 mm optical path.

2.7. Sample preparation for microscopy measurements

2.7.1. Buffer solutions

Buffer 1: 10 mM Hepes (> 99.5 Buffer grade, Carl-Roth Art.-Nr: HN07.1), 1 mM $MgCl_2$ (> 99 Cell pure, Carl-Roth Art.-Nr: HN78.2), 0.03% w/v β-DM (Lauryl-β-D-maltoside, > 99% for biochemistry, Art. CN26.2), pH = 7.8. Buffer 2: 10 mM Hepes, 1 mM $MgCl_2$, ~0.001% w/v β-DM, pH = 7.8. Buffer 3: 10 mM Hepes, 1 mM $MgCl_2$, ~6 μM β-DM, pH = 5.

2.7.2. Cleaning of cover slips

Glass coverslips (Menzel-glaser #1.5) were placed in a staining jar and rinsed 3 times with ultrapure water (LaboStar, Siemens). Water was exchanged with 1% Alconox detergent solution (Alconox powdered precision cleaner) and the jar sonicated for 10 min (Ultrasonic Cleaning Unit RK 102H, Bandelin). Detergent solution was discarded from the jar and rinsed 4 times with ultrapure water. Water was exchanged with isopropanol (2-propanol ≥ 99.5%, art.no.: 9866.6 Carl-Roth). Isopropanol was discarded and the jar with coverslips was vacuumed in the plasma machine (PDC-002, Harric plasma) for 20 min, then plasma etched at ~400 mTorr pressure using maximal power for 5 min.

2.7.3. Surface modification of coverslips and flowcell assembling

Clean glass coverslips were incubated with 0.01% of PLL (P4707 Sigma) for 10 min, then rinsed with ultrapure water, dried and assembled into the flowcell (sticky-slide VI 0.4, 80,608, IBIDI) with the PLL modified side facing the sticky slide. Tubings were inserted into the inlet and outlet port of the cell and channel was filled with buffer 1.

2.7.4. LHCII immobilization and imaging

Channel of the flow cell was filled with the buffer 1. ~1e + 06 diluted LHCII dissolved in buffer 1 were injected into the flowcell channel and incubated for 3 min. 300 μl of the buffer 1 was injected to wash out the excess of unbound LHCII. For microscopy 100 μl of buffer 1 containing 10 units/ml of pyranose oxidase (P4234, Sigma-Aldrich) and 300 units/ml catalase (C9322, Sigma-Aldrich), 1% glucose (ß-D-glucose, G0047, TCI, AMERICA). When exchanging the buffer conditions 300 μl of either buffer 2 or buffer 3 were injected and then 100 μl of the same buffer supplemented with oxygen scavengers was injected.

2.8. TIRF microscopy

The SM fluorescence microscopy set-up used in this study was essentially the same as described previously [33]. The 635 nm laser beam is expanded 13×. The 635 nm excitation intensity after the objective was 0.15 mW (< 10 W/cm^2 at the sample plane) and exposure time was 50 ms.

As previously, described all data analysis procedures were performed and graphs prepared in Igor Pro 6.37 (Wavemetrics, USA) program using custom written analysis package (available upon direct request to the author or under the link: http://www.igorexchange.com/project/TEA_MT) [33]. Only difference is that for the intensity change point (ICP) detection minimal amplitude now was set to 33 a.u. and the sum of the absolute slope values of the line fits of the states had to be smaller than a set value of 20. Additionally we have employed the *t*-test statistics to reject the putative ICPs – if t-value of the t-test for the ICP under revision was < 1.3, the ICP was rejected.

3. Results

3.1. Bulk fluorescence spectroscopy

Xanthophyll cycle carotenoids were found to be loosely bound to the V1 site of LHCII and to be easily lost upon purification procedures, but a mild solubilisation with the non-ionic detergent dodecyl-D-

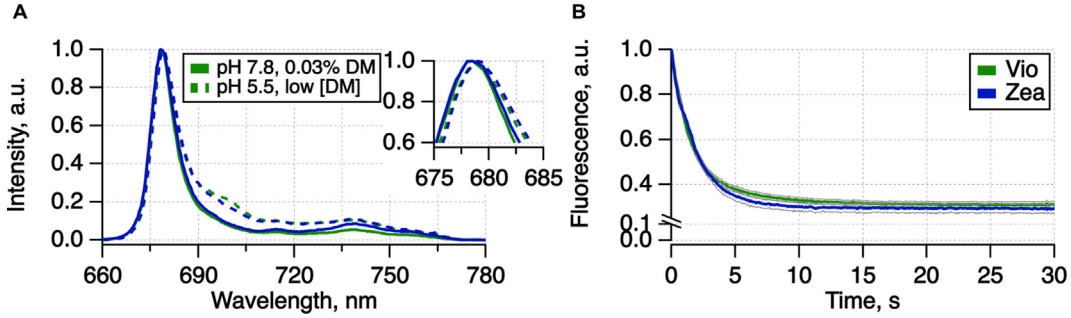

Fig. 2. Bulk fluorescence spectroscopy results of Vio and Zea-enriched LHCII samples and the effect of quenching induction in bulk. A) Fluorescence emission spectra measured at 77 K in high detergent and pH 7.8 (solid lines) as well as low detergent and pH 5.5 (dashed lines) conditions. Inset shows zoomed top of the main peak. B) Quenching induction traces of LHCII – intensity of chlorophyll fluorescence (integral of wavelength range > 700 nm), which was excited with a weak 635 nm light, versus time. Initially at the high detergent concentration and pH 7.8 LHCII solution was resuspended into low detergent and low pH buffer, resulting in the final detergent concentration of 6 μM and pH ~5.5. Maximum achieved quenching – decrease of the fluorescence intensity, was ~70% for both Vio- and Zea-enriched LHCII. The fluorescence traces were normalized at the beginning of the trace. Traces are the means of 4–8 replicates and grey lines represent the boundaries for standard error of means.

Table 1
Pigment composition of LHCII collected from sucrose gradients. DES = de-epoxidation state ((zeaxanthin + ½ antheraxanthin) * 100 / (violaxanthin + zeaxanthin + antheraxanthin)); Presented data is the mean of 3 replicates, and ± indicates st. dev.

Sample	Chl *a*/*b*	DES	%Vio/Car	%Zea/Car
Vio-enriched LHCII	1.48 ± 0.01	0	17.25 ± 0.82	0
Zea-enriched LHCII	1.42 ± 0.00	76.19 ± 1.52	3.84 ± 0.36	12.27 ± 0.29

maltoside can preserve well the intactness of these peripheral xanthophylls [29,30,34]. To isolate LHCII with the maximum amount of xanthophyll cycle carotenoids bound, thylakoids from either dark-adapted or light-treated spinach leaves were solubilized with a carefully determined β-dodecyl-D-maltoside (β-DM) concentration and loaded on sucrose gradients. The fraction of LHCII trimers (~0.3 M sucrose) was collected and the identity of the proteins was confirmed via absorption measured at room temperature (RT, SI Fig. 1) and low-temperature fluorescence analysis (Fig. 2A, SI Fig. 2). The pigment analysis showed a high de-epoxidation yield in the light-treated samples (around 76%, see Table 1) and a good retention of the xanthophyll cycle pigments in the purification procedure. The Chl *a*/*b* ratio was slightly higher than 8/6 = 1.33, that follows from the crystallographic data [4], because due to the isolation conditions we have also collected some (up to 10%) minor antennae complexes. However, this is a negligible amount of impurity and this procedure allowed us to achieve high de-epoxidation yield.

RT absorption spectra showed small red shift around 505 nm region of Zea sample, which is an independent indication of successful Zea enrichment. Meanwhile, fluorescence spectroscopy performed using streak camera at the RT under high detergent and high pH conditions showed that the fluorescence spectrum of the light-pretreated (Zea-enriched) LHCII trimers exhibits slightly less intense red shoulder of the spectrum (at ~720–740 nm) compared to the dark-pretreated (Vio-enriched) samples (see SI Fig. 3A–C). It was also noticed that the main peak of fluorescence spectrum is composed of two sub-peaks (centered at 686 and 689 nm), with the second sub-peak being more intense in the Zea-enriched LHCII, a characteristic conserved when measuring the emission at 77 K (data not shown). The whole fluorescence spectrum of Zea-enriched sample seems to be redshifted by several nm, compared to Vio-enriched ones. Fluorescence decay kinetics in both samples exhibited no dependence on the detection wavelength (see SI Fig. 3E–H) and were practically indistinguishable between the samples (SI Fig. 3D), with dominating lifetime component of ~3.5 ns and some fraction (~13%) of the faster component of ~0.6–0.8 ns (see SI Fig. 3 caption for the bi-exponential description). This indicates that the presence (or absence) of the red shoulder in the LHCII fluorescence spectrum is not related to the quenching mechanism [11,35].

Early studies on isolated LHCII complexes have shown that xanthophyll cycle carotenoids modulate the quenching induced by low pH, with Vio and Zea having inhibiting or enhancing effects, respectively, on the quenching kinetics [18,26]. This modulation shows conserved features in isolated chloroplasts and in leaves, suggesting that the xanthophyll cycle pool indeed controls the dynamics of qE by modulating the switch of a single antenna complex to a dissipative state. To explicitly determine the effect of different xanthophyll composition on the ability of LHCII complex to switch from a light-harvesting to a dissipative state, we measured intensity of chlorophyll fluorescence emission of LHCII samples versus time by re-suspending both samples, initially prepared at high detergent concentration and high pH buffer, into a buffer with low pH and low detergent concentration. The gradual decrease of the detergent concentration initiated the formation of mostly two-dimensional [11,36] LHCII aggregates, thus mimicking excitation energy transfer through the thylakoid membrane. At the same time, acidification of the buffer solution promoted the conformational switching of LHCIIs into the quenching state [37,38], resulting in the random generation of the NPQ traps within the LHCII aggregate.

The resulting quenching induction traces are shown in Fig. 2B. After ~25 s, the buffer re-suspending resulted in ~6 μM detergent concentration and pH 5.5 of the solution for both samples. This was accompanied by a significant change in the observed fluorescence intensity: initially, the absolute FL emission intensity in the Vio-enriched LHCIIs was by 15% smaller than in the Zea-enriched ones. Later on, during the injection of the buffer with low detergent concentration and low pH, the FL intensity dropped rapidly by (69.16 ± 1.37)% and (70.89 ± 1.97)% in the Vio- and Zea-enriched samples, respectively (± represents standard error from 4 to 8 replicates), indicating that LHCII complexes underwent a fast switch into the dissipative state. As we can see in Fig. 2B, upon normalizing the Fl quenching kinetics at the initial intensity, both samples reached the same final state, but the quenching induction was slightly faster in the Zea-enriched samples: there, the maximal fluorescence quenching was observed after ~10 s, whereas for Vio-enriched LHCIIs it took about 15 s. This difference may be related to the different aggregation rate of Vio- and Zea-enriched LHCII after the change in detergent concentration and pH conditions. This observation is in line with the previously published experimental works [18,25,45,26,27,39–44]. The differences we observed in our measurements were less evident than in the previous studies, because we were working with physiological amounts of xanthophyll cycle Cars bound to the native pocket of LHCII and not with the externally added

Cars. The quenching effect was less obvious and reached a similar extent, both in the Vio- and Zea-enriched LHCI samples. Therefore, Zea is unlikely to be a major quencher in LHCII.

To further investigate the (in)significance of the red shoulder in fluorescence spectrum and its relation to the fluorescence quenching, we also measured the steady-state fluorescence spectra of both samples at 77 K (Fig. 2A) and the fluorescence decay kinetics at the RT (SI Fig. 4) in the high detergent concentration and high pH (corresponding to the conditions at the beginning of the quenching traces shown in Fig. 2B) as well as in the low detergent concentration and low pH conditions (the final condition of the quenching traces). We can notice that the fluorescence spectra in high detergent concentration and high pH conditions exhibit the same features as the streak camera measurements (cf. Fig. 2A and SI Fig. 3C), but upon the change in buffer conditions we have observed an increase in the red shoulder intensity (at ~ 700 nm) for both samples. This is a well-known spectral indicator of the formation of LHCII aggregates [11,27,46,47]. In both aggregated samples, the spectra again are very similar, though the red shoulder is slightly more intense in the Vio-enriched LHCII samples. Also, upon the change in buffer conditions, both samples exhibited a slight red shift of the main peak (see inset in Fig. 2A). The measured fluorescence lifetime kinetics were fitted by the bi-exponential function and upon the change in buffer conditions of both samples they showed the shortening of both time components and increase in the shorter time component amplitude (Table 2). The average fluorescence lifetime decreased from 3.62 ns to 1.4 ns for Vio-enriched samples and from 3.53 ns to 1.55 ns for Zea-enriched ones.

To further investigate the effect of pH and detergent concentration on both Vio- and Zea-LHCII samples, we also studied them by means of single-molecule (SM) fluorescence microscopy. In this way, we were able to retrieve the fluorescence behavior of isolated LHCII in controlled condition while avoiding their aggregation. As a result, this approach allowed us to clarify whether the observed differences in ensembles (Fig. 2B) are due to intrinsic conformational single-protein dynamics or structural rearrangements of several complexes while LHCII aggregate is formed.

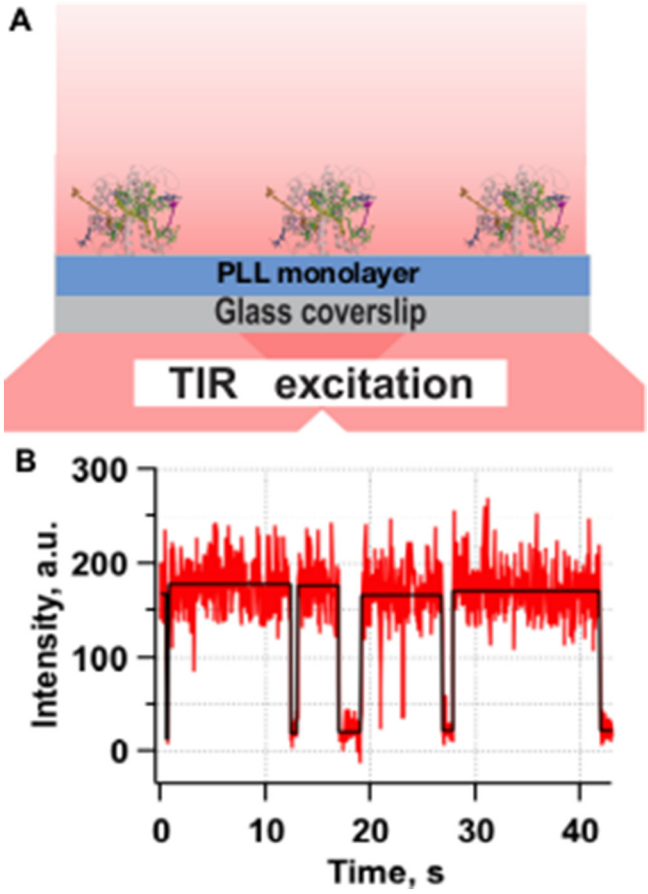

Fig. 3. A) Shematics of LHCII immobilization for SM TIRF microscopy measurements on the PLL coated glass coverslip. B) Illustrative SM trace - fluorescence emission intensity versus time. Horizontal lines indicate the resolved mean FL intensity levels that were used in further analysis.

3.2. Single-molecule microscopy

To investigate the conformational dynamics of single LHCII trimers, we have employed SM Total Internal Reflection Fluorescence (TIRF) microscopy. We have used this method recently to study single monomeric LHCII complexes lacking some particular carotenoids due to mutagenic sample preparation [28]. Here we have examined both Vio- and Zea-enriched LHCII samples solubilized in detergent micelles immobilized on PLL coated-glass coverslip at low densities (Fig. 3A) under the 635 nm wavelength excitation and 50 ms exposition time. From the acquired movies we have extracted fluorescence intensity variations over time and selected those spots representing single LHCII complexes (Fig. 3B). These fluorescence time traces exhibit a well-known blinking behavior [38,48] due to reversible switching of the pigment–protein complexes between the strongly- and weakly-fluorescing states as a result of the conformational dynamics of protein scaffold [37]. By overlapping similar FL time traces measured for 438 distinct LHCII trimers, we obtain the two-dimensional map shown in Fig. 4A and representing time-dependent distribution of various detected FL intensity levels. Since only those LHCII trimers initially being in strongly emitting state were detected, there was relatively small number of quenched complexes during the first second. At later times, due to reversible switching into the non-fluorescent state and irreversible photobleaching the population of zero-intensity level increases. After ~30 s of continuous illumination the majority of LHCII complexes were bleached irreversibly.

The discussed FL intensity map shown in Fig. 4A was obtained from the Vio-enriched LHCII complexes under the buffer conditions mimicking the light-harvesting state (pH 7.8, high detergent concentration). Similar data were also acquired for the Zea-enriched complexes (Fig. 4B) as well as both Vio- and Zea-enriched trimers under buffer condition imitating the high-light acclimation (pH 5.5 and low detergent concentration), see Fig. 4C and D respectively. The intermediate conditions of high pH and low detergent concentration are shown in SI Fig. 5. By visually comparing these FL intensity maps we can note that detergent removal alone produces much smaller effect than when

Table 2
Bi-exponential description ($F(t) = A_1\exp(-t/\tau_1) + A_2\exp(-t/\tau_2)$) of the fluorescence decay kinetics in Vio- and Zea-enriched LHCII trimers before and after quenching induction shown in SI Fig. 4.

Sample	A_1 (%)	τ_1 (ns)	A_2 (%)	τ_2 (ns)	$< \tau >$ (ns)
Vio-enriched LHCII, pH 7.8, 0.03% DM	93	3.78 ± 0.01	7	1.54 ± 0.1	3.62
Zea-enriched LHCII, pH 7.8, 0.03% DM	90	3.74 ± 0.02	10	1.67 ± 0.08	3.53
Vio-enriched LHCII, pH 5.5, low [DM]	63	1.73 ± 0.01	37	0.85 ± 0.02	1.4
Zea-enriched LHCII, pH 5.5, low [DM]	55	1.93 ± 0.02	45	1.08 ± 0.02	1.55

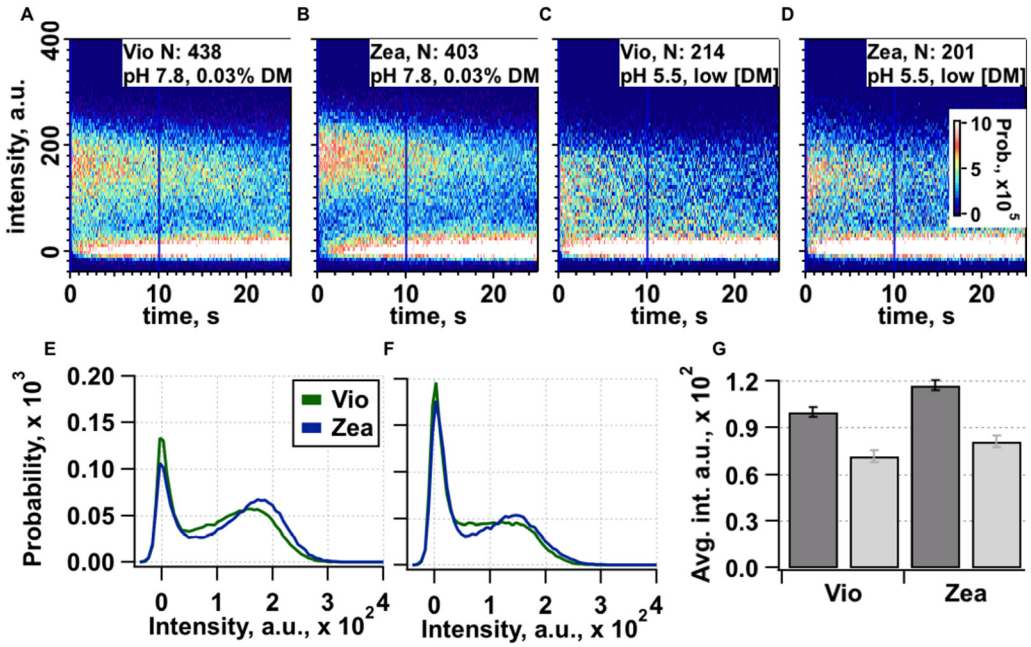

Fig. 4. Single-molecule population emission plots in Vio- and Zea-enriched LHCII trimers (A–D) and their vertical linescans for the initial 10 s (E and F). Panels A, B and E correspond to the high detergent and high pH conditions, panels C, D and F – to the low detergent and low pH conditions. G) Average intensity of population of SM traces from 0 till 10 s. Black – high detergent high pH conditions, grey – low detergent low pH. Number of included molecules in each plot are indicated on the top right corner of panels A–D.

accompanied with the acidification of the buffer solution: while the former factor does not lead to any pronounced re-distribution of the FL intensities, the latter one results in considerably faster photobleaching and, more importantly, the formation of additional conformational states with intermediate FL intensities. That can be easily seen from the FL intensity histograms shown in Fig. 4E–F and SI Fig. 5C that were obtained by integrating FL maps from Fig. 4A–D and SI Fig. 5A–B over the first 10 s, when most of the trimers are still active. By describing these histograms as a sum of Gaussian peaks, each possibly corresponding to a distinct conformational state, we were able to distinguish at least three such states: the non-fluorescent state S1, intermediate fluorescent state S2, and highly fluorescent state S3.

We see from Fig. 4 that under light-harvesting conditions (high detergent concentration and high pH value) Zea-enriched complexes exhibit slightly higher probability to be in the highly fluorescent state compared to the Vio-enriched ones. As already mentioned, reduction of the detergent concentration of the buffer (while still keeping high pH value) does not result in any significant differences in the distribution of FL intensities, suggesting that detergent concentration alone does not influence conformational dynamics of the LHCII complexes. On the other hand, under low detergent concentration and low pH conditions the probability of the highly fluorescent state is notably reduced at the expense of the increased probabilities for both non-fluorescent and intermediate states. These changes are accompanied with the FL intensity shift of the highly fluorescent state towards the lower values. Overall, upon lowering both detergent concentration and pH values there is a considerable (by ~30%) drop in the mean FL intensity in both Vio- and Zea-enriched LHCII complexes (see Fig. 4G). Interestingly, by comparing both samples we can also note that the Vio-enriched complexes exhibit slightly higher probability to be in the non-fluorescent state than the Zea-enriched ones (cf. Fig. 4E–F). As a result, in the light-harvesting-mimicking conditions the mean FL intensity in the Zea-enriched complexes is by ~20% *larger* than in the Vio-enriched trimers (compare dark bars in Fig. 4G). This value is similar to the mentioned ~15% (p-value < 0.05) difference in the absolute FL intensity, observed between Vio- and Zea-enriched samples in bulk measurements. On the other hand, at low pH the difference in mean FL intensities in both samples becomes less pronounced (see light bars in Fig. 4G).

There is a possibility that upon reduction of detergent concentration and pH level some fraction of the surface-immobilized LHCII complexes became permanently strongly quenched and therefore undetectable by the automated analysis. To estimate the percentage of such undetectable complexes, we calculated the average number of fluorescent spots per image in each step of the experiment (SI Fig. 6). Since the sole drop in the detergent concentration does not promote the conformational quenched state of LHCII, we attributed the observed ~ 10% decrease in the average number of the detected spots per image to unbinding of LHCII from the surface due to the washing step. On the other hand, once both detergent concentration and pH level were reduced to mimic NPQ conditions, the number of detected spots per image farther decreased by 25%-that could be the results of either somewhat weaker binding of the LHCII complexes to the PLL surface in acidic environment (and therefore more pronounced washing off) or the switching of these LHCII complexes into long-living strongly quenched state, so that they did not exhibit any conformational dynamics and remained too dim for the detection during the whole measurement. However, even in the later less probable scenario accounting to these undetected LHCII trimers would increase the fluorescence intensity drop observed in our SM analysis to ~ 50%, which is still far from a 70% decrease in fluorescence intensity observed in the aggregated state in bulk.

To further analyze the time traces of FL intensity variations, we have applied the Intensity Change Point (ICP) detection algorithm that allows characterization of the correlation between the detected FL intensity level (state of constant fluorescence emission) and its duration before transition to another intensity level occurs. The resulting correlation maps, obtained for different samples and different buffer conditions are shown in Fig. 5A–D. We see that most probable dwell times between the subsequent transitions were smaller than 2 s, though sometimes LHCII trimer remained at the same FL intensity for as long as 15 s. The mean duration of the dark or dim (FL intensities below 20 a.u.), intermediate (from 20 to 130 a.u.) or highly fluorescing (above 130 a.u.) are presented in Fig. 5E–F and are rather identical for both Vio- and Zea-enriched samples. On average, highly fluorescent states lasted about 3 times shorter than the dim states, and the intermediate states were even shorter. The reduction of detergent concentration and pH level leads mainly to the shortening of the intermediate state and increased probability for the dim state at the expense of highly fluorescing state.

In addition to changes revealed by the state intensity–duration correlation plot, the pathways of the transition between different states could also be affected. These can be accessed by constructing the

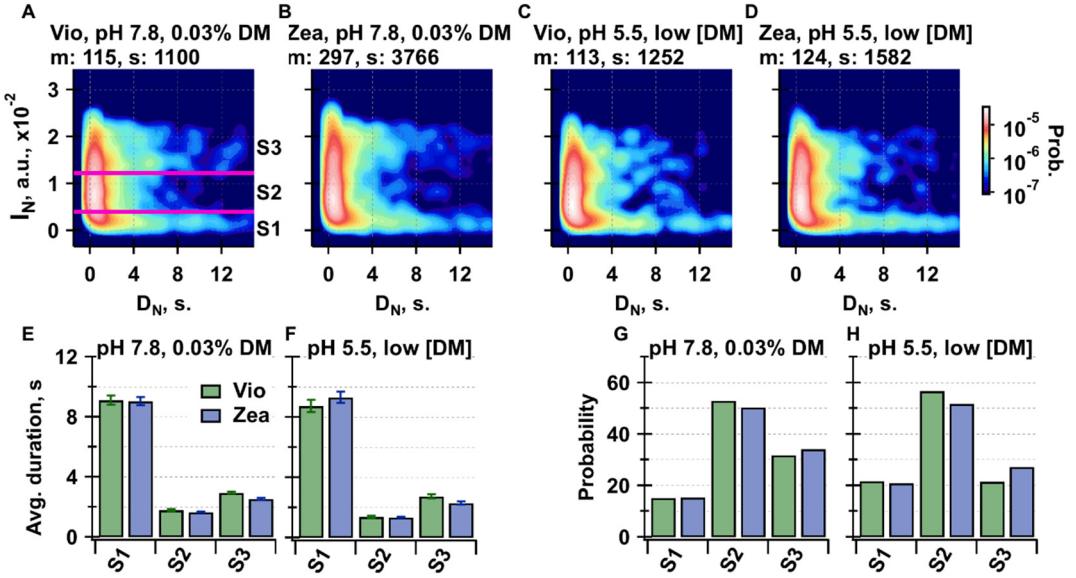

Fig. 5. State intensity versus duration plots. A–B) high detergent high pH, C–D) low detergent low pH. I_N – average intensity of state N, D_N – average duration of state N. Number of included molecules (m) and detected intensity states (s) are indicated at the top of each graph. Plots are normalized to their total area. Logarithmic color scale represents probability density. E–F) average durations and G–H) probabilities of non-fluorescent (S1) and fluorescent (S2 and S3) states.

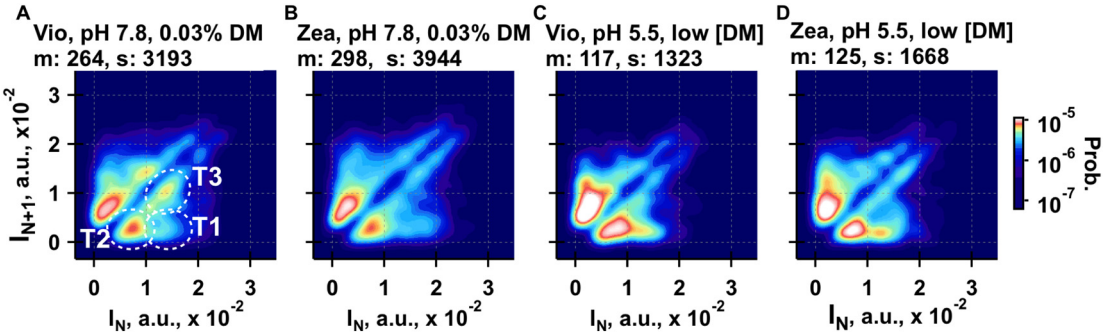

Fig. 6. Transition density plots. A–B) high detergent high pH, C–D) low detergent low pH conditions. I_N – average intensity of state N, I_{N+1} – average intensity of state N + 1. Number of included molecules (m) and states (s) are indicated above each graph. Plots are normalized to probability density function. Logarithmic color scale represents probability.

transition density maps, where the x-axis corresponds to the FL intensity I_N of some resolved level (state of constant fluorescence emission) in the acquired SM fluorescence intensity time trace shown in Fig. 3B, while y-axis—that of the subsequent (in time) intensity level I_{N+1}. The resulting maps for different samples and different buffer conditions are presented in Fig. 6. All of these maps are quite dispersed with several dominating transitions. For example in the Fig. 6A there are three main transitions: T1 – between the strongly fluorescing state and the non-fluorescent state, T2 – between the intermediate intensity state and the non-fluorescent state, T3 – between the high intensity state and intermediate one. Differently from our previously studied monomeric LHCII complexes from the Lut-deficient mutants [33], all these transition maps are essentially symmetrical with respect to the diagonal, meaning that the forward and backward transitions between some particular intensity levels are approximately equally probable. In other word, the free energies of different conformational states corresponding to these intensity levels are very similar. At the high detergent concentration and high pH conditions, both samples showed the mentioned three dominating transitions T1, T2 and T3. The only difference between the samples was the probability of these transitions: T3 transition was more probable in the Vio-enriched sample. Upon the lowering of detergent concentration and pH level, in the Vio-enriched LHCII complexes the probability of T3 transition became similar to T1, while probability of T2 notably increased. Again, the Zea-enriched trimers exhibited almost the same transition density pattern. This property supports that both samples at low pH possess the same quenching ability.

4. Discussion

In this work, we have compared the spectral signatures of LHCII complexes gently isolated from the dark-adapted or light-treated thylakoids, in order to retain the maximum amount of xanthophyll cycle carotenoids (Table 1). Our results show that a selective enrichment of LHCII with violaxanthin or zeaxanthin does not affect the ability of LHCII to switch to a dissipative conformation or the maximum quenching inducible. In these samples, environmental changes that mimic qE conditions (pH decrease and detergent removal) results in the identical ~70% drop in the fluorescence intensity, which suggests that presence of Zea is not essential for the excitation quenching (Fig. 2B). However, the kinetics of the fluorescence decrease due to NPQ induction are different, prompting towards a modulatory effect of zeaxanthin in the dynamics of quenching.

The physical origin of the observed 70%-drop of the fluorescence intensity upon the pH decrease and detergent removal is two-fold: first, variation of the environment conditions naturally affects the conformational dynamics of the pigment–protein, making its quenching state thermodynamically more favorable. Meanwhile, further drop of

fluorescence intensity results from the formation of aggregates, which stabilizes the quenched conformation and allows excitation energy transfer through the aggregate towards the LHCII complexes being in the quenched state. In order to distinguish between these two different processes—conformational dynamics and aggregation effects—we have implemented SM microscopy technique and studied single immobilized LHCII complexes. We observed that the mere removal of detergent influence conformational dynamics of the LHCIIs in a much less pronounced way than when accompanied with acidification of the environment (cf. Fig. 3 and SI Fig. 6). In SM experiments LHCIIs are surface-immobilized at low densities and therefore, in contrast to the typical bulk measurements, their aggregation upon removing the detergent is prevented. Another effect that the detergent concentration reduction alone might induce is the conformational change of LHCII. Thus in SM experiments low detergent concentration and high pH control is more beneficial than a high detergent concentration low pH control because it allows decoupling the conformational change effect from aggregation. Moreover, in the SM microscopy measurements we observed ~30%-drop in the mean fluorescence intensity after mimicking NPQ conditions. That means that the remaining 40%-drop detected during the bulk measurements originates from the LHCII aggregation. Therefore, slight increase in the quenching induction rate in the Zea-enriched samples, observed during the bulk fluorescence measurements (Fig. 2B) suggests that Zea, locating the peripheral binding site of the LHCII protein, might play mediating role enhancing the aggregation process. It is worthwhile to mention that these findings agree well with the results of the previously published SM level studies of Vio- and Zea-enriched LHCII, which showed that at the SM level both types of the enriched samples can achieve maximum average fluorescence decrease of ~35% [49].

In addition to these findings, by comparing the steady-state fluorescence spectra and the excitation decay kinetics of Vio- and Zea-enriched LHCII complexes, we can conclude that the presence or absence of the red shoulder in the steady state fluorescence spectrum (see SI Fig. 3C) is not directly related to the quenching state of the LHCII complexes: despite slight spectral differences, both samples exhibited virtually the same excitation decay kinetics (SI Fig. 3D). This is in line with our recent studies, showing that red-shifted emission, originating from chlorophyll-chlorophyll charge transfer states, exhibits a strong temperature dependence and is not linked to the quenching mechanism [11,35].

We have also provided evidence of rather subtle differences of the main Chl fluorescence peak (the presence of two sub-peaks of the top of the main peak, and red-shifting of the whole spectrum) between Zea- and Vio-LHCII. This internal structure of the fluorescence spectra cannot be separated by taking different vertical or horizontal sections of the streak camera images, indicating that these features are convolved. Indeed, complex state-transition patterns revealed by the SM data might be related to this complex internal structure of the fluorescence spectra. In a previous work, excitation fluorescence spectra of thylakoids enriched in zeaxanthin showed that there is a weak coupling between Zea and Chls [50]. It has been recently proposed that structural changes associated with qE bring about a stronger coupling between Chl and Zea, which allow for dissipative processes to occur with the direct participation of Zea [51]. Our findings on the presence of a red-shifted fluorescence emission peak suggest that there is a weak effect of Zea on the terminal emitter site. However, this effect does not change the dynamics of quenched and unquenched states of LHCII, as shown by the single molecule spectroscopy data, suggesting that whether Zea is weakly coupled to chlorophylls or simply its binding provokes slight changes in the arrangement of other pigments, it is probably not involved in the quenching process. The structure of LHCII binding zeaxanthin is currently unavailable, and this result in difficulties in determining its coupling strength to other pigments [16,52].

Finally, we detected that while variations of the buffer condition affect the protein's conformational dynamics, neither the state-duration nor transition density plots showed major differences between the quenching abilities of both Vio- and Zea-enriched LHCII samples, again suggesting that Zea does not directly participates in excitation quenching. Moreover, from Fig. 2C we can see that under typical low-light conditions (i.e. high pH level) the presence of Zea results in stronger fluorescence compared to the Vio-samples, that might even reduce the unnecessary loss of excitation energy.

Together with PsbS protein, zeaxanthin is a crucial modulator of the NPQ process [53]. Our single-molecule study considers the two extremes of unquenched and quenched conformation and shows that there are no differences in the presence of violaxanthin or zeaxanthin. The quenching level observed during the ensemble measurements is in good agreement with these findings, showing that the extent of quenching inducible in isolated LHCII upon acidification and detergent removal is the same. The differences are found in the quenching induction *kinetics*, which show a faster decay of the fluorescence yield of Zea-enriched LHCII and strongly support the role of zeaxanthin as an allosteric modulator of the quenching process. The most likely mechanistic explanation considers a structural effect of zeaxanthin that promotes faster LHCII clustering in virtue of its markedly hydrophobic nature and position at the interface between LHCII trimers [3,25,54]. Aggregation of LHCII in the thylakoid membrane arises as a consequence of a conformational switch of the LHCII and in turn stabilizes the dissipative state [55]. Endogenous levels of either violaxanthin or zeaxanthin were found to inhibit or promote LHCII aggregation, respectively [18]. The marked hydrophobic nature of zeaxanthin could also bring to a change of the pKa of some amino acids important for the conformational switch, making LHCII more sensitive to protonation [25,56].

Whether PsbS and Zea play a synergetic role in the modulation of quenching, is still unclear [57,58]. However, even if both promote the LHCII aggregation in thylakoids during high light [55,59], their role in the relaxation of NPQ is seemingly different [60]. While PsbS is acting as a fast switch that allows for quick kinetics of formation and relaxation of the quencher, the de-epoxidation of violaxanthin has a rather opposite effect, being activated relatively slowly and persisting in the dark, delaying the recovery of chlorophyll fluorescence [53]. The relevance of this difference is to be found in the adaptation of plants to sun-flecks and fast changes in sunlight intensities, when PsbS-mediated prompt response of the regulation of the photosynthetic machinery is essential together with the establishment of a zeaxanthin-induced “memory of illumination history” [25], whereby the photosynthetic membrane is more prone to the dissipation of excess, potentially harmful excitation energy.

Transparency document

The Transparency document associated this article can be found, in online version.

Acknowledgment

This work was supported by the European Union's Horizon 2020 research and innovation programme under the Marie Skłodowska-Curie grant agreement (No. 675006) and Gilibert project funded by Lithuanian Research Council (No. S-LZ-19-3).

Appendix A. Supplementary data

Supplementary data to this article can be found online at https://doi.org/10.1016/j.dummy.2019.01.002.

References

[1] B. Demmig-Adams, G. Garab, W. Adams, Govindjee. Non-Photochemical Quenching and Energy Dissipation in Plants, Algae and Cyanobacteria. 40, Springer,

Netherlands, 2014.
[2] P. Horton, A.V. Ruban, R.G. Walters, Regulation of light harvesting in green plants, Annu. Rev. Plant Physiol. Plant Mol. Biol. 47 (1996) 655–684.
[3] A.V. Ruban, M.P. Johnson, C.D.P. Duffy, The photoprotective molecular switch in the photosystem II antenna, Biochim. Biophys. Acta Bioenerg. 1817 (2012) 167–181.
[4] X.-P. Li, et al., A pigment-binding protein essential for regulation of photosynthetic light harvesting, Nature 403 (2000) 391–395.
[5] C. Funk, et al., The PSII-S protein of higher plants: a new type of pigment-binding protein, Biochemistry 34 (1995) 11133–11141.
[6] B. Demmig-Adams, Carotenoids and photoprotection in plants: a role for the xanthophyll zeaxanthin, BBA-Bioenergetics 1020 (1990) 1–24.
[7] N.E. Holt, et al., Carotenoid cation formation and the regulation of photosynthetic light harvesting. *Science (80-.)*, vol. 307, (2005), pp. 433–436.
[8] A.V. Ruban, et al., Identification of a mechanism of photoprotective energy dissipation in higher plants, Nature 450 (2007) 575–578.
[9] S. Bode, et al., On the regulation of photosynthesis by excitonic interactions between carotenoids and chlorophylls, Proc. Natl. Acad. Sci. 106 (2009) 12311–12316.
[10] T.K. Ahn, et al., Architecture of a charge-transfer state regulating light harvesting in a plant antenna protein. Science (80-.), vol. 320, (2008), pp. 794–797.
[11] J. Chmeliov, et al., The nature of self-regulation in photosynthetic light-harvesting antenna, Nat. Plants 2 (2016) 16045.
[12] L. Dall'Osto, et al., Two mechanisms for dissipation of excess light in monomeric and trimeric light-harvesting complexes, Nat. Plants 3 (2017) 17033.
[13] A.J. Townsend, et al., The causes of altered chlorophyll fluorescence quenching induction in the Arabidopsis mutant lacking all minor antenna complexes, Biochim. Biophys. Acta Bioenerg. 1859 (2018) 666–675.
[14] Z. Liu, et al., Crystal structure of spinach major light-harvesting complex at 2.72 Å resolution, Nature 428 (2004) 287–292.
[15] N.I. Bishop, The β,ε-carotenoid, lutein, is specifically required for the formation of the oligomeric forms of the light harvesting complex in the green alga, scenedesmus obliquus, J. Photochem. Photobiol. B Biol. 36 (1996) 279–283.
[16] J. Chmeliov, et al., An 'all pigment' model of excitation quenching in LHCII, Phys. Chem. Chem. Phys. 17 (2015) 15857–15867.
[17] K.F. Fox, et al., The carotenoid pathway: what is important for excitation quenching in plant antenna complexes? Phys. Chem. Chem. Phys. 19 (2017) 22957–22968.
[18] A. Ruban, P. Horton, The xanthophyll cycle modulates the kinetics of non-photochemical energy dissipation in isolated light-harvesting complexes, intact chloroplasts, and leaves of spinach, Plant Physiol. 119 (1999) 531–542.
[19] D.I. Sapozhnikov, T.A. Krasovskaya, A.N. Maevskaya, Change in the interrelationship of the basic carotenoids of the plastids of green leaves under the action of light, Dokl Akad Nauk USSR 113 (1957).
[20] H.Y. Yamamoto, T.O.M. Nakayama, C.O. Chichester, Studies on the light and dark interconversions of leaf xanthophylls, Arch. Biochem. Biophys. 97 (1962) 168–173.
[21] H.A. Frank, et al., Photophysics of the carotenoids associated with the xanthophyll cycle in photosynthesis, Photosynth. Res. 41 (1994) 389–395.
[22] T. Polivka, J.L. Herek, D. Zigmantas, H.-E. Akerlund, V. Sundstrom, Direct observation of the (forbidden) S1 state in carotenoids, Proc. Natl. Acad. Sci. 96 (2002) 4914–4917.
[23] S. Park, et al., Chlorophyll-carotenoid excitation energy transfer in high-light-exposed thylakoid membranes investigated by snapshot transient absorption spectroscopy, J. Am. Chem. Soc. 140 (2018) 11965–11973.
[24] P. Horton, A.V. Ruban, M. Wentworth, Allosteric regulation of the light-harvesting system of photosystem II, Philos. Trans. R. Soc. Lond. Ser. B Biol. Sci. 355 (2000) 1361–1370.
[25] A.V. Ruban, M.P. Johnson, Xanthophylls as modulators of membrane protein function, Arch. Biochem. Biophys. 504 (2010) 78–85.
[26] A.V. Ruban, A. Young, P. Horton, Modulation of Chlorophyll Fluorescence Quenching in Isolated Light Harvesting Complex of Photosystem II, *BBA - Bioenerg.* **1186** (1994), pp. 123–127.
[27] A.V. Ruban, D. Phillip, A.J. Young, P. Horton, Carotenoid-dependent oligomerization of the major chlorophyll a/b light harvesting complex of photosystem II of plants, Biochemistry 36 (1997) 7855–7859.
[28] T.P.J. Krüger, C. Ilioaia, M.P. Johnson, A.V. Ruban, R. Van Grondelle, Disentangling the low-energy states of the major light-harvesting complex of plants and their role in photoprotection, Biochim. Biophys. Acta Bioenerg. 1837 (2014) 1027–1038.
[29] P. Xu, L. Tian, M. Kloz, R. Croce, Molecular insights into zeaxanthin-dependent quenching in higher plants, Sci. Rep. 5 (2015).
[30] A.V. Ruban, P.J. Lee, M. Wentworth, A.J. Young, P. Horton, Determination of the stoichiometry and strength of binding of xanthophylls to the photosystem II light harvesting complexes, J. Biol. Chem. 274 (1999) 10458–10465.
[31] D. Rees, et al., pH dependent chlorophyll fluorescence quenching in spinach thylakoids from light treated or dark adapted leaves, Photosynth. Res. 31 (1992) 11–19.
[32] K. Petrou, E. Belgio, A.V. Ruban, PH sensitivity of chlorophyll fluorescence quenching is determined by the detergent/protein ratio and the state of LHCII aggregation, Biochim. Biophys. Acta Bioenerg. 1837 (2014) 1533–1539.
[33] M. Tutkus, J. Chmeliov, D. Rutkauskas, A.V. Ruban, L. Valkunas, Influence of the carotenoid composition on the conformational dynamics of photosynthetic light-harvesting complexes, J. Phys. Chem. Lett. 8 (2017) 5898–5906.
[34] S. Caffarri, R. Croce, J. Breton, R. Bassi, The major antenna complex of photosystem II has a xanthophyll binding site not involved in light harvesting, J. Biol. Chem. 276 (2001) 35924–35933.
[35] A. Gelzinis, J. Chmeliov, A.V. Ruban, L. Valkunas, Can red-emitting state be responsible for fluorescence quenching in LHCII aggregates? Photosynth. Res. 135 (2018) 275–284.
[36] J. Chmeliov, G. Trinkunas, H. van Amerongen, L. Valkunas, Excitation migration in fluctuating light-harvesting antenna systems, Photosynth. Res. 127 (2016) 49–60.
[37] L. Valkunas, J. Chmeliov, T.P.J. Krüger, C. Ilioaia, R. Van Grondelle, How photosynthetic proteins switch, J. Phys. Chem. Lett. 3 (2012) 2779–2784.
[38] T.P.J. Krüger, C. Ilioaia, R. van Grondelle, Fluorescence intermittency from the main plant light-harvesting complex: resolving shifts between intensity levels, J. Phys. Chem. B 115 (2011) 5071–5082.
[39] D. Phillip, A.V. Ruban, P. Horton, A. Asato, A.J. Young, Quenching of chlorophyll fluorescence in the major light-harvesting complex of photosystem II: a systematic study of the effect of carotenoid structure, Proc. Natl. Acad. Sci. 93 (1996) 1492–1497.
[40] A.V. Ruban, D. Phillip, A.J. Young, P. Horton, Excited-state energy level does not determine the differential effect of violaxanthin and zeaxanthin on chlorophyll fluorescence quenching in the isolated light-harvesting complex of photosystem II, Photochem. Photobiol. 68 (1998) 829–834.
[41] M. Wentworth, A.V. Ruban, P. Horton, Chlorophyll fluorescence quenching in isolated light harvesting complexes induced by zeaxanthin, FEBS Lett. 471 (2000) 71–74.
[42] M.P. Johnson, P.A. Davison, A.V. Ruban, P. Horton, The xanthophyll cycle pool size controls the kinetics of non-photochemical quenching in Arabidopsis thaliana, FEBS Lett. 582 (2008) 262–266.
[43] M. Wentworth, A.V. Ruban, P. Horton, Kinetic analysis of nonphotochemical quenching of chlorophyll fluorescence. 2. Isolated light-harvesting complexes, Biochemistry 40 (2001) 9902–9908.
[44] A.V. Ruban, A.J. Young, P. Horton, Dynamic properties of the minor chlorophyll a/b binding proteins of photosystem II, an in vitro model for photoprotective energy dissipation in the photosynthetic membrane of green plants, Biochemistry 35 (1996) 674–678.
[45] A.V. Ruban, D. Rees, A.A. Pascal, P. Horton, Mechanism of ΔpH-dependent dissipation of absorbed excitation energy by photosynthetic membranes. II. The relationship between LHCII aggregation in vitro and qE in isolated thylakoids, BBA-Bioenergetics 1102 (1992) 39–44.
[46] A.V. Ruban, J.P. Dekker, P. Horton, R.V.A.N. Grondelle, Temperature dependence of chlorophyll fluorescence from the light harvesting complex II of higher plants, Photochem. Photobiol. 61 (1995) 216–221.
[47] N.M. Magdaong, M.M. Enriquez, A.M. LaFountain, L. Rafka, H.A. Frank, Effect of protein aggregation on the spectroscopic properties and excited state kinetics of the LHCII pigment–protein complex from green plants, Photosynth. Res. 118 (2013) 259–276.
[48] G.S. Schlau-Cohen, et al., Single-molecule identification of quenched and unquenched states of LHCII, J. Phys. Chem. Lett. 6 (2015) 860–867.
[49] T.P.J. Krüger, et al., The specificity of controlled protein disorder in the photoprotection of plants, Biophys. J. 105 (2013) 1018–1026.
[50] C. Ilioaia, C.D.P. Duffy, M.P. Johnson, A.V. Ruban, Changes in the energy transfer pathways within photosystem II antenna induced by xanthophyll cycle activity, J. Phys. Chem. B 117 (2013) 5841–5847.
[51] S. Park, et al., Snapshot transient absorption spectroscopy of carotenoid radical cations in high-light-acclimating thylakoid membranes, J. Phys. Chem. Lett. 8 (2017) 5548–5554.
[52] C.D.P. Duffy, et al., Modeling of fluorescence quenching by lutein in the plant light-harvesting complex LHCII, J. Phys. Chem. B 117 (2013) 10974–10986.
[53] A.V. Ruban, Nonphotochemical chlorophyll fluorescence quenching: mechanism and effectiveness in protecting plants from photodamage, Plant Physiol. 170 (2016) 1903–1916.
[54] P. Horton, A.V. Ruban, A.J. Young, Regulation of the structure and function of the light harvesting complexes of photosystem II by the xanthophyll cycle, The Photochemistry of Carotenoids, Kluwer Academic Publishers, 2006, pp. 271–291.
[55] M.P. Johnson, et al., Photoprotective energy dissipation involves the reorganization of photosystem II light-harvesting complexes in the grana membranes of spinach chloroplasts, Plant Cell 23 (2011) 1468–1479.
[56] E.L. Mehler, M. Fuxreiter, I. Simon, E. Garcia-Moreno, B. The role of hydrophobic microenvironments in modulating pKa shifts in proteins, Proteins Struct. Funct. Genet. 48 (2002) 283–292.
[57] M. Aspinall-O'Dea, et al., In vitro reconstitution of the activated zeaxanthin state associated with energy dissipation in plants, Proc. Natl. Acad. Sci. 99 (2002) 16331–16335.
[58] V. Daskalakis, Protein–protein interactions within photosystem II under photoprotection: the synergy between CP29 minor antenna, subunit S (PsbS) and zeaxanthin at all-atom resolution, Phys. Chem. Chem. Phys. 20 (2018) 11843–11855.
[59] M.A. Ware, V. Giovagnetti, E. Belgio, A.V. Ruban, PsbS protein modulates non-photochemical chlorophyll fluorescence quenching in membranes depleted of photosystems, J. Photochem. Photobiol. B Biol. 152 (2015) 301–307.
[60] E.J. Sylak-Glassman, et al., Distinct roles of the photosystem II protein PsbS and zeaxanthin in the regulation of light harvesting in plants revealed by fluorescence lifetime snapshots, Proc. Natl. Acad. Sci. 111 (2014) 17498–17503.